Quasi-Reflectionless Short-Through-Line-Based Bandstop Filters

Adnan Nadeem, *Student Member, IEEE*, Symeon Nikolaou, *Senior Member, IEEE*, Photos Vryonides, *Senior Member, IEEE*, and Dimitra Psychogiou, *Senior Member, IEEE*

***Abstract*—Highly miniaturized input quasi-reflectionless bandstop filters (BSFs) are reported. They are based on a complementary RF diplexer design approach where the bandstop branch is formed by cascaded short-through-line (STL)-based bandstop stages and the bandpass branch by a single first-order bandpass filter (BPF). When compared to conventional input quasi-reflectionless BSFs, the proposed approach leads to a significantly smaller size for multistage implementations. The operating principles of the STL-based BSF concept are provided through circuit-simulated examples demonstrating scalability in terms of bandwidth (BW) and selectivity. For validation purposes, the single- and two-stage microstrip prototypes were built and tested at 2 GHz. The single-stage prototype exhibits: center frequency (f_0): 2 GHz, stopband rejection: 25 dB, 3-dB stopband BW: 135 MHz (6.75%), and 10-dB input return-loss (RL) BW: 2 GHz. The two-stage prototype demonstrates: (f_0): 2 GHz, stopband rejection >35 dB, 3-dB stopband BW: 228 MHz (11.4%), and 10-dB RL BW: 2 GHz.**

***Index Terms*—Bandstop filter (BSF), complementary-diplexer, phase shifter, reflectionless.**

I. Introduction

Bandstop filters (BSFs) are present in practically every wireless communication and radar system, aiming to reject co-site and adjacent-channel interference by reflecting the RF signal energy back to the source. Recently, new types of quasi-reflectionless or absorptive BSFs [1], [2], [3], [4], [5], [6], [7], [8] have been introduced to absorb the reflected RF signal energy thereby improving the overall signal-to-noise of the RF front-end by canceling multireflections that would otherwise lead to instabilities and intermodulation. In [1], a transmission-line-based quasi-reflectionless BSF was reported using short- and open-circuited sections to achieve broadband matching (DC–5f_0, where f_0 is the center frequency). Quasi-reflectionless BSFs employing symmetric routing and folded-line structures were introduced in [2], where resistively terminated bandpass filter (BPF) branches were used to maintain the reflectionless condition over a wide frequency span (1.36–3.5 GHz). Multilayer implementations exhibiting wide reflectionless behavior (DC–1.2f_0) were demonstrated in [3], having relatively large physical size ($0.33\lambda_g \times 1.43\lambda_g$). In yet another approach, balanced quasi-reflectionless BSFs with differential-/common-mode absorption were reported in [4]. Adaptive reflectionless BSF concepts have also been shown. Specifically, in [5], tunable complementary networks were integrated in the BSF to preserve low input reflection under reconfigurable operating conditions. This principle has been widely adopted in subsequent studies [6], [7], [8] to develop reflectionless and absorptive filtering networks.

Despite the significant RF performance advancements demonstrated by reflectionless BSFs to date, they are large in size due to: 1) requiring additional one or two resistively terminated BPF sections of the same order as the main BSF signal path; 2) their BSF branch being based on a long-through-line implementation where series (or inverted parallel) resonators are connected on a long-through-line [$(N+2)\cdot 90°$, where N is the filter order] between the RF input and output of the filter in quarter-wavelength intervals resulting in a large physical size when high rejection levels are required.

To overcome these limitations, this work explores the potential to realize highly miniaturized quasi-reflectionless BSFs using miniaturized short-through-line (STL)-based BSF branches and first-order resistively loaded bandpass branches. When compared to conventional reflectionless BSFs, the proposed approach leads to a significantly smaller size for multistage implementations due to being based on short interconnecting lines (<90°) and dual-coupled resonators. To the best of the authors' knowledge, the application of the STL dual-coupled resonator concept to the realization of quasi-reflectionless BSF is uniquely shown in this work for the first time in terms of design and practical validation. Scalability to higher order transfer functions without increasing the order of the auxiliary bandpass branches, leading to smaller size implementations when compared to conventional reflectionless BSFs (see [2], [4]), and arbitrary stopband bandwidths (BWs) are also uniquely demonstrated. As proof-of-concept, two microstrip prototypes were uniquely designed, manufactured, and tested.

II. Theoretical Foundations

A. STL Quasi-Reflectionless BSF Stage

The conceptual block diagram of the proposed quasi-reflectionless STL-based BSF is shown in Fig. 1(a) for its basic single-stage realization. It is based on a complementary-diplexer approach comprising a BSF branch and a resistively

Received 31 March 2026; accepted 3 April 2026. This work was supported in part by the BRIDGE2HORIZON/0823D/0007 (KAREFLECT) and BRIDGE2HORIZON/0823D/25 (RF_NEXT GEN) Projects through the Cohesion Policy Funds under Grant THALEIA 2021-2027 and in part by the Research Ireland under Grant 20/RP/8334. *(Corresponding author: Dimitra Psychogiou.)*

Adnan Nadeem, Symeon Nikolaou, and Photos Vryonides are with the Frederick Research Center, Frederick University, 1036 Nicosia, Cyprus (e-mail: anadeem.msee19rimms@seecs.edu.pk; s.nikolaou@frederick.ac.cy; p.vryonides@frederick.ac.cy).

Dimitra Psychogiou is with the University College Cork, Cork 21, T12 K8AF Ireland, and also with Tyndall National Institute, Cork, T12 R5CP Ireland (e-mail: dpsychogiou@ucc.ie).

This article was presented at the IEEE MTT-S International Microwave Symposium (IMS 2026), Boston, MA, USA, June 7–12, 2026.

Digital Object Identifier 10.1109/LMWT.2026.3681467

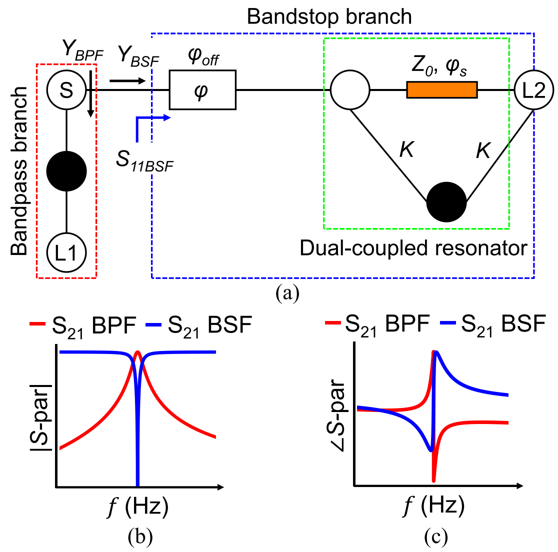

Fig. 1. (a) Block diagram of the single-stage quasi-reflectionless BSF based on a complementary-diplexer configuration comprising an STL-based BSF and an auxiliary BPF branch. Conceptual power transmission response in (b) magnitude and (c) phase of the BPF and the BSF branch.

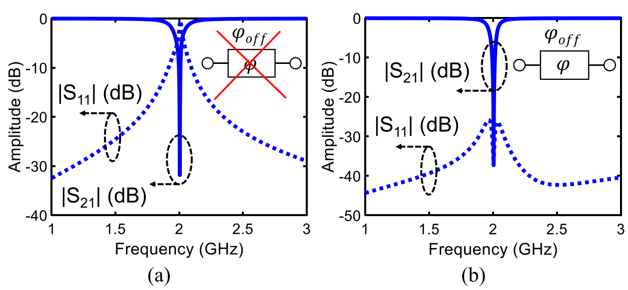

Fig. 2. Theoretical S-parameters of the single-stage quasi-reflectionless STL BSF in Fig. 1: (a) without and (b) with phase offset (φ_s = 20°, φ_{off} = 80°, and K = 0.3).

loaded auxiliary BPF branch. Their corresponding conceptual power transmission response in terms of magnitude and phase is, respectively, shown in Fig. 1(b) and (c). The BSF branch is based on a first-order implementation that comprises: 1) an STL of electrical length φ_s and characteristic impedance Z_0, with $\varphi_s < 90°$; and 2) a dual-coupled resonator that is coupled by two admittance inverters with admittance K. The STL-based BSF is designed using the methodology in [9] and [10], where K relates to the effective inverter (K_{eq}) seen by its equivalent single-coupled resonator by the standard microwave-network relationship

$$K_{\mathrm{eq}} = \sqrt{2}K^2(1 + \cos\varphi_s) \quad (1)$$

and therefore governs the resulting stopband BW. For a chosen φ_s, the K values are then calculated using the exact single- and dual-coupled transformation in [9]. Furthermore, the auxiliary BPF branch is designed for a first-order response and is resistively loaded. In this manner, the RF input signal power in the stopband of the STL-based BSF is dissipated in the loading resistor instead of being reflected at the input. To achieve the input-reflectionless characteristics, the BPF and BSF branches need to have complementary responses as shown in Fig. 1

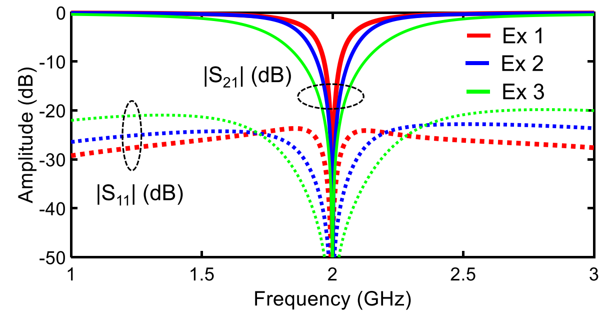

Fig. 3. Theoretical S-parameters of the single-stage quasi-reflectionless STL-based BSF demonstrating BW reconfigurability. Ex.1: $K = 0.3, \varphi_s = 20°$, and φ_{off} = 80°. Ex.2: $K = 0.39, \varphi_s = 25°$, and φ_{off} = 77.5°. Ex.3: $K = 0.43$, φ_s = 30°, and φ_{off} = 75°.

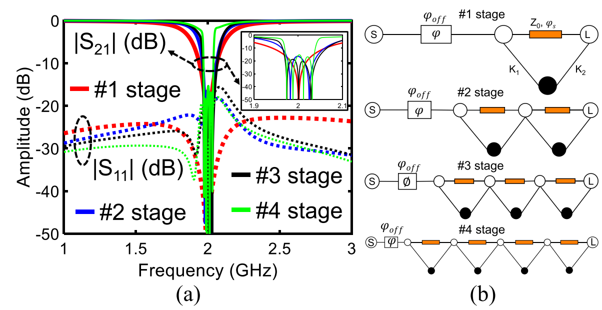

Fig. 4. Scalability of the STL quasi-reflectionless BSF with increasing number of stages. (a) Ideally synthesized S-parameters for one-, two-, three-, and four-stage STL BSF. (b) Corresponding circuit topologies of the one-, two-, three-, and four-stage STL quasi-reflectionless BSF implementations (φ_s = 20°).

and discussed in [5] so that their input admittances meet as follows:

$$\overline{Y_{BSF}}(\omega) + \overline{Y_{BPF}}(\omega) \approx 1 \quad \forall\omega \quad (2)$$

which is equal to 1 at the center frequency (f_0). However, due to the BSF being based on an STL, the phase of its input admittance is shifted in relation to that of a conventional BSF, requiring a phase-compensation block with a phase φ_{off} to be included in its input that needs to fulfill as follows:

$$\varphi_{off} + \frac{\varphi_s}{2} = 90° \quad (3)$$

which is derived by setting the phase of the reflection coefficient at the input of the bandstop branch in the following equation:

$$\angle S_{11BSF} = 180° - \phi_s - 2\phi_{off} \quad (4)$$

equal to zero. To demonstrate the effect of the phase-compensation mechanism, a comparison of the STL-based BSF response without and with the phase-compensation block is illustrated in Fig. 2(a) and (b), respectively. As can be seen, when the phase offset is present, the input quasi-reflectionless characteristics are obtained. Without the phase offset, the admittances of the two branches do not align, completely losing the quasi-reflectionless characteristic.

B. BW and Selectivity

Fig. 3 illustrates the BW reconfigurability capabilities of the proposed quasi-reflectionless STL BSF for three different coupling configurations (Ex.1–Ex.3). Each example corresponds to a distinct set of K inverter values, which are provided in the caption of Fig. 3. Increasing K enhances the coupling

This article has been accepted for inclusion in a future issue of this journal. Content is final as presented, with the exception of pagination.

TABLE I
COMPARISON WITH STATE-OF-THE-ART QUASI-REFLECTIONLESS BSFs

Ref.	**Type**	***f₀* (GHz)**	***N***	**3-dB BW (MHz)**	**10-dB RL-BW (GHz)**	**Stopband rejection (dB)**	**Size (λ_gx λ_g)**
[2]	Two-port	2.35	2	280	2.19	>60	1.89 x 1.08
[4]	Two-port	1.99	2	159	2	>25	2.0 x 1.3
[6]	One-port	1.93	3	245	1.6	>35	1.7 x 1.57
[8]	One-port	2	2	150	1.57	>15	1.29 x 1.28
T.W	One-port	2	1	135	2	>25	0.24 x 0.44
T.W	One-port	2	2	228	2	>35	0.35 x 0.42

N: number of stages, 3-dB BW: 3-dB absolute stopband BW, 10-dB RL-BW: 10-dB input return loss BW ($|S_{11}| < -10$ dB), T.W: this work

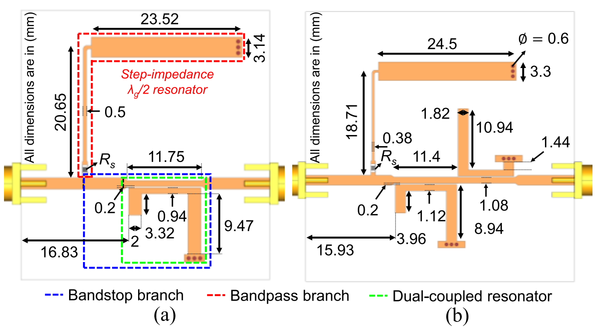

Fig. 5. Layouts of the quasi-reflectionless STL-based BSF prototypes. (a) Single-stage STL-based BSF and (b) two-stage STL-based implementations, $R_s = 50\ \Omega$.

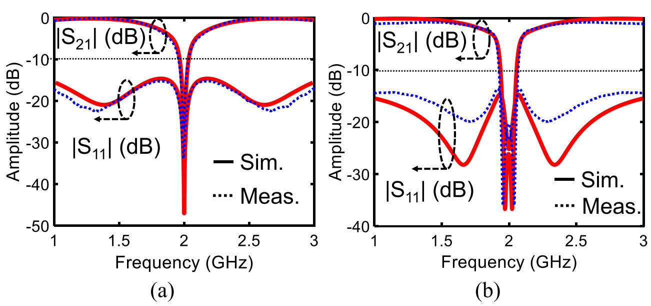

Fig. 6. RF-measured and EM-simulated S-parameters. (a) Single-stage quasi-reflectionless STL-based BSF. (b) Two-stage quasi-reflectionless STL-based BSF.

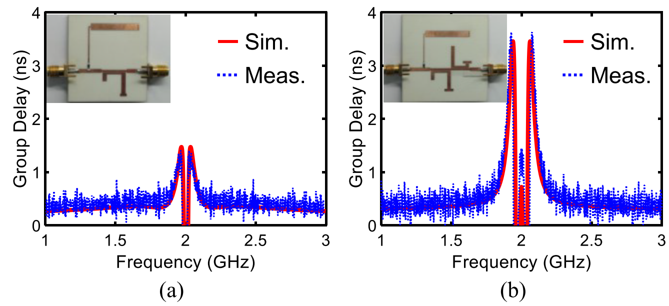

Fig. 7. RF-measured and EM-simulated group-delay responses with the inset showing the manufactured prototypes of (a) single-stage STL-based BSF and (b) two-stage STL-based BSF.

between the resonator and the STL and therefore results in a wider stopband BW as observed in Ex.3. It should be noted that in all of these examples, the phase offset condition in (3) is met, ensuring that $|S_{11}|$ remains low regardless of the selected BW. Fig. 4 shows how the stopband selectivity is improved as the number of the cascaded STL BSF stages increases from one to four. Noticeably, in all these examples, a single-phase offset block (with the exact same phase as in the single stage) is used at the front of the entire system to ensure the reflectionless condition and is independent of filter order. This is a key advantage of the proposed concept in relation to multistage realizations, allowing to increase selectivity by cascading electrically smaller BSF branches while using a single resistively terminated first-order BPF at the RF input.

III. EXPERIMENTAL VALIDATION

For proof-of-concept demonstration purposes, two microstrip-type single- and two-stage STL-based BSF prototypes were designed and manufactured for a center frequency of 2.0 GHz, and a φ_s is equal to 25°. Their design was performed using the design guidelines in Section II, using dual-coupled quarter-wavelength resonators in the BSF branch that facilitate further size compactness and a wide spur-free response. The BPF branch is implemented using a resistively loaded half-wavelength-long-step impedance resonator that is loaded with a resistor $R_s = 50\ \Omega$ at the junction where the BPF connects to the BSF, as shown in Fig. 5. A similar approach was discussed in [11]. The resistor can also be alternatively placed at the output of the BPF. For prototype realization, a Rogers RO4003C substrate ($\varepsilon_r = 3.38$, tan$\delta = 0.0027$, and thickness = 0.813 mm) was employed. The measured S-parameters and group-delay responses are presented in Figs. 6 and 7, respectively, while the photographs of the manufactured prototypes are shown in the inset of Fig. 7. As observed, a close agreement between the EM-simulated and RF-measured responses is achieved, successfully validating the proposed STL-based BSF concept. The overall electrical sizes of the single- and two-stage prototypes correspond to $0.24\lambda_g \times 0.44\lambda_g$ and $0.35\lambda_g \times 0.42\lambda_g$, respectively, where λ_g is the guided wavelength at 2 GHz. The measured characteristics of the single-stage STL BSF are summarized as follows. A well-defined stopband notch centered at 2 GHz is achieved with a rejection level of approximately 26.7 dB. The 3-dB absolute stopband BW is 135 MHz, corresponding to a 6.75% relative BW. The minimum passband insertion loss is 0.55 dB. The filter also exhibits a 10-dB input return-loss (RL) BW of approximately 2 GHz, demonstrating the intended input quasi-reflectionless behavior. The minimum input-matching levels within the 3-dB stopband and across the broader 1–3-GHz frequency span are 15.21 and 17.37 dB, respectively.

The measured RF performance metrics for the two-stage prototype are given as follows. The two transmission zeros are observed at 1.955 and 2.04 GHz, yielding rejection levels close to 35.8 dB. The 3-dB absolute stopband BW is 228 MHz, representing an 11.4% relative BW. A minimum passband insertion loss of 0.85 dB is obtained. Furthermore, it maintains a 10-dB input RL BW of approximately 2 GHz. The minimum in-band matching levels within the 3-dB stopband and over the 1–3-GHz span are 13.66 and 14.4 dB, respectively.

Table I compares the performance of the proposed STL-based BSF with representative state-of-the-art reflectionless BSFs. As can be seen, the previously reported absorptive BSFs typically occupy significantly larger areas (between $1.29\lambda_g \times 1.28\lambda_g$ and $1.89\lambda_g \times 1.57\lambda_g$ for second- or third-stage implementations, respectively), with 3-dB absolute stopband BWs of 150–280-MHz and 10-dB RL BWs between 1.57 and 2.19 GHz. The proposed single- and two-stage prototypes achieve comparable or higher stopband rejection levels while having a significantly reduced area ($0.24\lambda_g \times 0.44\lambda_g$ and $0.35\lambda_g \times 0.42\lambda_g$, respectively), representing nearly an order-of-magnitude miniaturization relative to existing quasi-reflectionless BSFs.

IV. Conclusion

This work presents a new class of miniaturized quasi-reflectionless BSFs using a complementary-diplexer architecture where the bandstop branch is formed by cascaded STL-based bandstop stages and the bandpass branch by a single first-order BPF. When compared to conventional input quasi-reflectionless BSFs, the proposed approach leads to a significantly smaller size for multistage implementations. The operating principles of the STL-based BSF concept are provided through circuit-simulated examples demonstrating scalability in terms of BW and selectivity, and are validated experimentally at 2 GHz through the implementation and testing of single- and two-stage prototypes.

References

[1] J. Lee and J. Lee, "Transmission-line absorptive bandstop filters with wide passband: Synthesis and design," *IEEE Trans. Microw. Theory Techn.*, vol. 69, no. 12, pp. 5371–5380, Dec. 2021, doi: 10.1109/TMTT.2021.3116083.

[2] R. Gómez-García, J.-M. Muñoz-Ferreras, and D. Psychogiou, "Symmetrical quasi-reflectionless BSFs," *IEEE Microw. Wireless Compon. Lett.*, vol. 28, no. 4, pp. 302–304, Apr. 2018, doi: 10.1109/LMWC.2018.2805462.

[3] J.-K. Xiao and J. Pu, "Synthesis of absorption reflectionless bandstop filter and its design using multi-layer self-packaged SCPW," *IEEE Access*, vol. 8, pp. 218803–218812, 2020, doi: 10.1109/ACCESS.2020.3042617.

[4] X.-B. Zhao, F. Wei, L. Yang, and R. Gómez-García, "Two-layer-magic-T-based bandpass, quasi-bandstop, and dual-passband balanced filters with differential-/Common-mode reflectionless behavior," *IEEE Trans. Microw. Theory Techn.*, vol. 72, no. 4, pp. 2267–2282, Apr. 2024, doi: 10.1109/TMTT.2023.3308390.

[5] D. Psychogiou and R. Gómez-García, "Reflectionless adaptive RF filters: Bandpass, bandstop, and cascade designs," *IEEE Trans. Microw. Theory Techn.*, vol. 65, no. 11, pp. 4593–4605, Nov. 2017, doi: 10.1109/TMTT.2017.2734086.

[6] R. Gómez-Garcia, J.-M. Muñoz-Ferreras, and D. Psychogiou, "High-order input-reflectionless bandpass/bandstop filters and multiplexers," *IEEE Trans. Microw. Theory Techn.*, vol. 67, no. 9, pp. 3683–3695, Sep. 2019, doi: 10.1109/TMTT.2019.2924975.

[7] J. Lee and J. Lee, "Arbitrary-order distributed-element narrowband reflectionless bandstop filter with canonical transmission response and broadband matching," *IEEE Trans. Microw. Theory Techn.*, vol. 68, no. 10, pp. 4381–4389, Oct. 2020, doi: 10.1109/TMTT.2020.3011164.

[8] R. Gomez-Garcia, J.-M. Munoz-Ferreras, W. Feng, and D. Psychogiou, "Input-reflectionless negative-group-delay bandstop-filter networks based on lossy complementary duplexers," in *IEEE MTT-S Int. Microw. Symp. Dig.*, Boston, MA, USA, Jun. 2019, pp. 1031–1034, doi: 10.1109/MWSYM.2019.8700887.

[9] A. C. Guyette and E. J. Naglich, "Short-through-line bandstop filters using dual-coupled resonators," *IEEE Trans. Microw. Theory Techn.*, vol. 64, no. 2, pp. 459–466, Feb. 2016, doi: 10.1109/TMTT.2015.2506631.

[10] E. J. Naglich, A. C. Guyette, and S. Shin, "Microwave bandstop filters with minimum through-line length," in *IEEE MTT-S Int. Microw. Symp. Dig.*, Phoenix, AZ, USA, May 2015, pp. 1–4, doi: 10.1109/MWSYM.2015.7166739.

[11] X. Wu, Y. Li, and X. Liu, "High-order dual-port quasi-absorptive microstrip coupled-line bandpass filters," *IEEE Trans. Microw. Theory Techn.*, vol. 68, no. 4, pp. 1462–1475, Apr. 2020.